Supplementary information for: PVA/AgNPs hydrogel SERS substrate combined with machine learning for highly sensitive detection of organic selenium species

Huaqing Ling[1,2,3], Zhixi Zhao[1,2,3,*], Ziqi Zhang[1,2,3], Shan Chen[1,2,3], Zulihaya Maimaiti[1,2,3]

[1]College of Chemistry and Chemical Engineering, Xinjiang Normal University, Urumqi 830054, China

[2]Xinjiang Key Laboratory of Energy Storage and Photoelectroctalytic Materials, Urumqi 830054, China

[3]Technical Research Center for Environmental Geotechnical Engineering Restoration and Resource Utilization, Xinjiang Normal University, Urumqi 830054, China

[*]Corresponding authors

Zhixi Zhao, College of Chemistry and Chemical Engineering, Xinjiang Normal University, Urumqi 830054, China. E-mail Address: zhixizhao@xjnu.edu.cn

Table of contents

1. SERS performance evaluation index

EF was a critical metric for evaluating the efficiency of substrate SERS. The calculation formula for the EF of the PVA/AgNPs hydrogel SERS substrate was provided as follows:

$$EF = \frac{I_{SERS}}{N_{SERS}} \times \frac{N_{NR}}{I_{NR}} \quad \text{(S1)}$$

I_{SERS} denoted the Raman signal intensity measured for organic selenium at a concentration of 5.78×10^{-6} mol/L (500 μg/L) after its interaction with the PVA/AgNPs hydrogel substrate. N_{SERS} represented the number of effective organic selenium molecules on the surface of the PVA/AgNPs hydrogel substrate that were irradiated by the light spot. I_{NR} corresponded to the Raman signal intensity of organic selenium at a concentration of 1 mol/L, while N_{NR} indicated the number of effective organic selenium molecules irradiated by the light spot.

2. Machine learning algorithms

Classification and recognition. The hyperparameter optimization for the four classification models, including PLS-DA, PCA-DA, KNN, and SVM, employed a combined strategy of five-fold cross-validation and grid search. The principal component numbers (PCs) for PCA-DA were directly determined based on cumulative variance contribution ≥95%. The latent variable numbers (LVs) for PLS-DA were optimized within the range of 1 to 15 by minimizing cross-validation error rates. The number of nearest neighbors (k) for KNN was selected from {3, 5, 7, 9, 11} to achieve the highest cross-validation accuracy, using Euclidean distance as the metric and weighted by the reciprocal of the distance. SVM employed a radial basis function (RBF) kernel. The penalty factor (C) and kernel parameter (γ) for the SVM model were optimized via grid search on a $\log_2$ scale. The search ranges were set to [2^{-5}, 2^{15}] for C and [2^{-15}, 2^{5}] for γ, to maximize cross-validation accuracy. The final selected optimal parameters and corresponding performance metrics were presented in Table S4.

The formulas used to calculate the performance evaluation metrics—accuracy, sensitivity, specificity, and precision—are provided below:

$$Accuracy = 100 \times \frac{TN}{TN + TP} \tag{S2}$$

$$Sensitivity = 100 \times \frac{TP}{TP + FN} \tag{S3}$$

$$Specificity = 100 \times \frac{TN}{TN + FP} \tag{S4}$$

$$Precision = 100 \times \frac{TP}{TP + FP} \tag{S5}$$

TP represented correct identification of positive samples. TN indicated correct identification of negative samples. FP referred to misclassification of negative samples as positive. FN denoted misclassification of positive samples as negative.

Quantitative analysis. The PLSR model was optimized using five-fold cross-validation to minimize RMSE, with LVs selected within the range of 1 to 15. For SVR, an RBF kernel was employed. The C and γ were optimized via grid search on a $\log_2$ scale within the range [2^{-15}, 2^{15}]. Three-fold cross-validation was used to minimize MSE, and the loss function parameter (ϵ) was fixed at 0.001. The final optimal parameters and corresponding prediction performance were summarized in Table S5. RMSE minimization served as the objective function. RMSE quantified the degree of dispersion between the predicted and true values, and a lower RMSE indicated higher prediction accuracy. MAE assessed the absolute magnitude of prediction errors. The R^2 quantified the proportion of concentration variance explained by the model. Combined, these metrics established a robust modeling framework for accurate organic selenium quantification in complex systems. The calculation formula is as follows:

$$RMSE = \sqrt{\frac{1}{n}\sum_{i=1}^{n}(y_i - \hat{y}_i)^2} \tag{S6}$$

Here, y_i represented the true value of the i -th observation, $\hat{y}_i$ denoted the predicted value of the i -th observation, and n indicates the total number of observations.

$$R^2 = 1 - \frac{\sum_{i=1}^{n}(y_i - \hat{y}_i)^2}{\sum_{i=1}^{n}(y_i - \bar{y})^2} \tag{S7}$$

Here, $\bar{y}_i$ denoted the mean of all observed values.

$$MAE = \frac{1}{n}\sum_{i=1}^{n}\left|y_i - \hat{y}_i\right| \tag{S8}$$

3. Optimization of PVA/AgNPs hydrogel SERS substrate.

To optimize the performance of the PVA/AgNPs hydrogel SERS substrate, we systematically investigated the effect of AgNPs concentration. Silver nanosols with concentrations of 0.10% w/v, 0.15% w/v, and 0.20% w/v were synthesized. Among them, the 0.20% w/v AgNPs exhibited the most intense plasmon resonance absorption in the UV-Vis spectra (Fig. S3a). However, in the SERS detection of SeMet, the substrate with 0.15% (w/v) AgNPs yielded the highest signal enhancement at the characteristic peaks of 640 cm^{-1} and 827 cm^{-1} (Fig. S3b). Excessive aggregation of AgNPs occurred at 0.20% w/v concentration. This aggregation reduced the number of effective SERS "hot spots" and modified molecular adsorption configurations. Consequently, detection sensitivity was compromised despite increased overall absorbance. The 0.15% w/v AgNPs concentration was selected as the optimal formulation. This concentration achieved an optimal compromise between electromagnetic field enhancement and molecular adsorption environment. The balanced performance established the most suitable conditions for the detection system.

The volume ratio between PVA gel and AgNPs was systematically optimized to evaluate effects on SERS substrate enhancement performance. SERS detection of 500 μg/L SeMet was conducted using volume ratios of 1:1, 2:1, 2:3, 3:1, and 3:2. As depicted in Fig. S3c and Fig. S3d, the 3:1 ratio produced the maximum intensity for the characteristic Raman peak of SeMet among all conditions tested. This optimal performance was attributed to the synergistic interplay between the quantity of PVA gel, the dispersion state, and the efficiency of hot spot formation in the AgNPs. A 3:1 ratio enabled the PVA gel to form a stable three-dimensional network. This structure effectively dispersed and immobilized AgNPs, preventing nanoparticle aggregation and deactivation. Concurrently, the configuration promoted generation of densely distributed, readily accessible SERS hot spots. The 2:1 ratio resulted in an insufficient gel volume for effective AgNPs dispersion and hot spot generation. Both 2:3 and 3:2 ratios further weakened the protective function. These suboptimal conditions collectively compromised hot spot stability and overall signal enhancement efficiency. At a 1:1 ratio, the minimal amount of gel was insufficient to effectively inhibit the aggregation and oxidation of AgNPs. Consequently, the number of hot spots was dramatically reduced alongside a decrease in their activity, ultimately leading to the weakest signal enhancement capability. Therefore, a 3:1 volume ratio of PVA gel to AgNPs was identified as the optimal formulation for constructing the SERS substrate, ensuring effective analyte enrichment and maximized utilization of SERS hot spots.

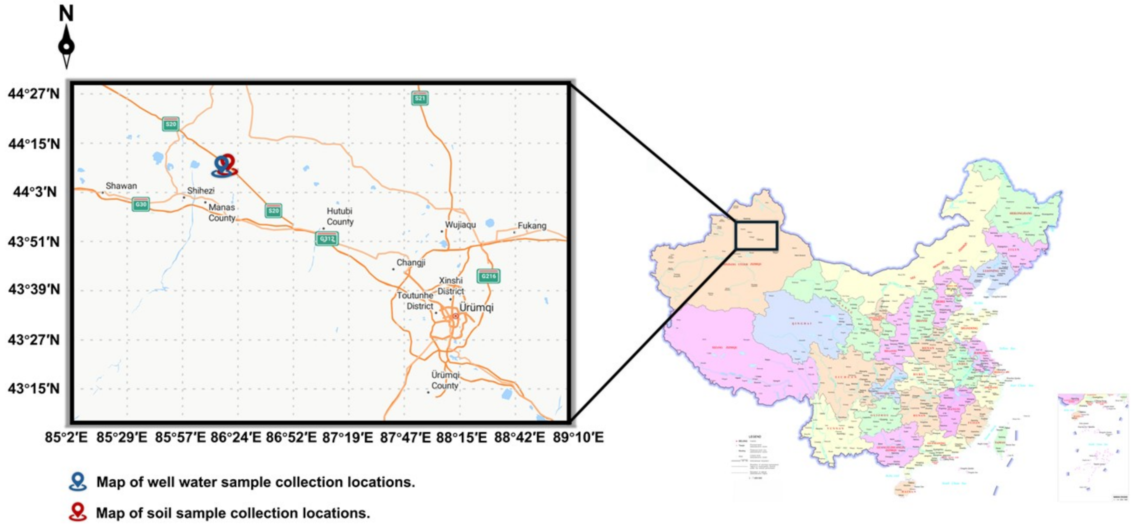

Fig. S1 Maps showing the locations of the real samples collected for the study.

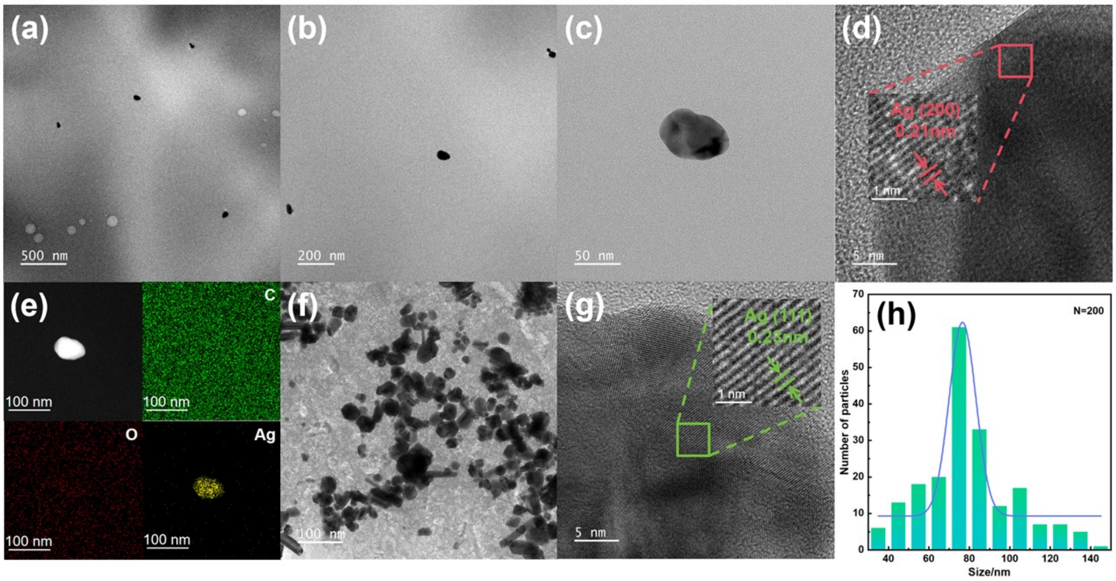

Figure S2 (a–d) HR-TEM images of PVA/AgNPs at different scales. (e) Elemental mapping of PVA/AgNPs at 100 nm scale. HR-TEM images of AgNPs sol at (f) 100 nm and (g) 5 nm scales. (h) Particle size distribution histogram of AgNPs.

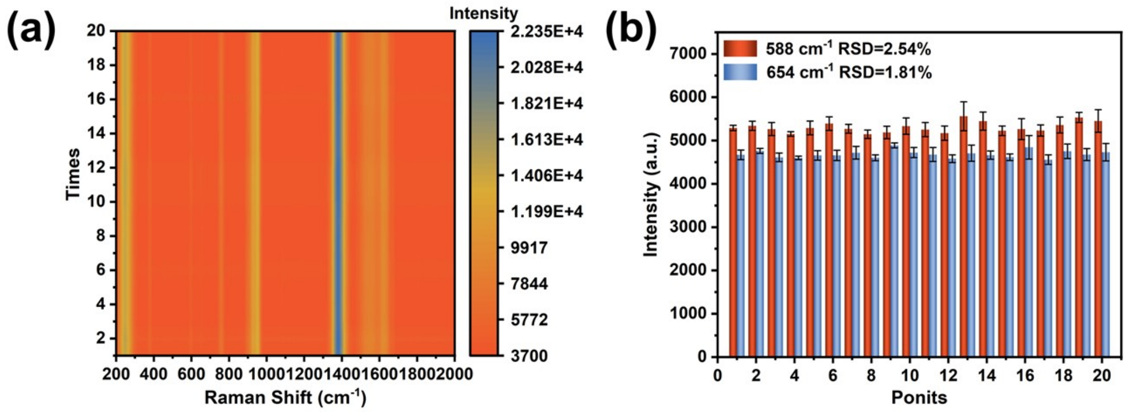

Fig. S3 The homogeneity of the SERS substrate was evaluated by (a) spectral mapping and (b) characteristic peak RSD of SeMCys.

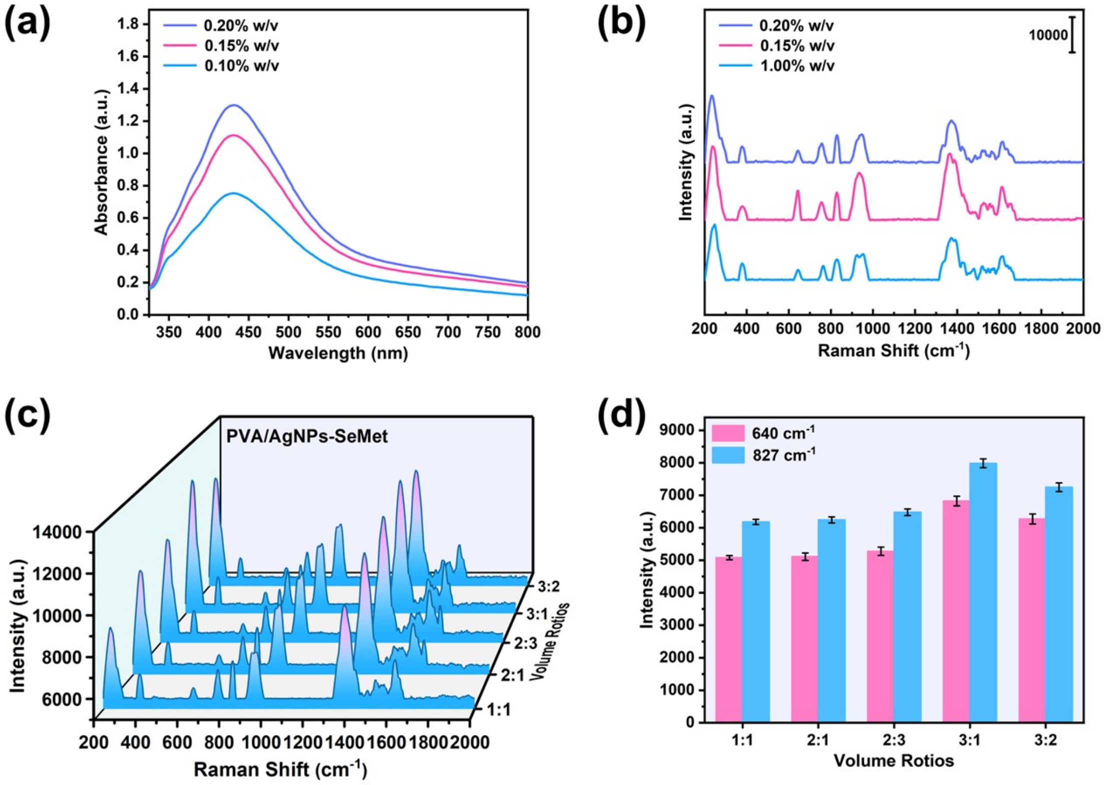

Fig. S4 (a) UV-vis spectra of AgNPs at different concentrations. (b) SERS spectra of 500 μg/L SeMet were detected by different concentrations of AgNPs. (c) Three-dimensional SERS spectra with optimized volume ratio of PVA gel to AgNPs. (d) The variation of SeMet characteristic peak intensity with volume ratio at 640 cm^{-1} and 827 cm^{-1}.

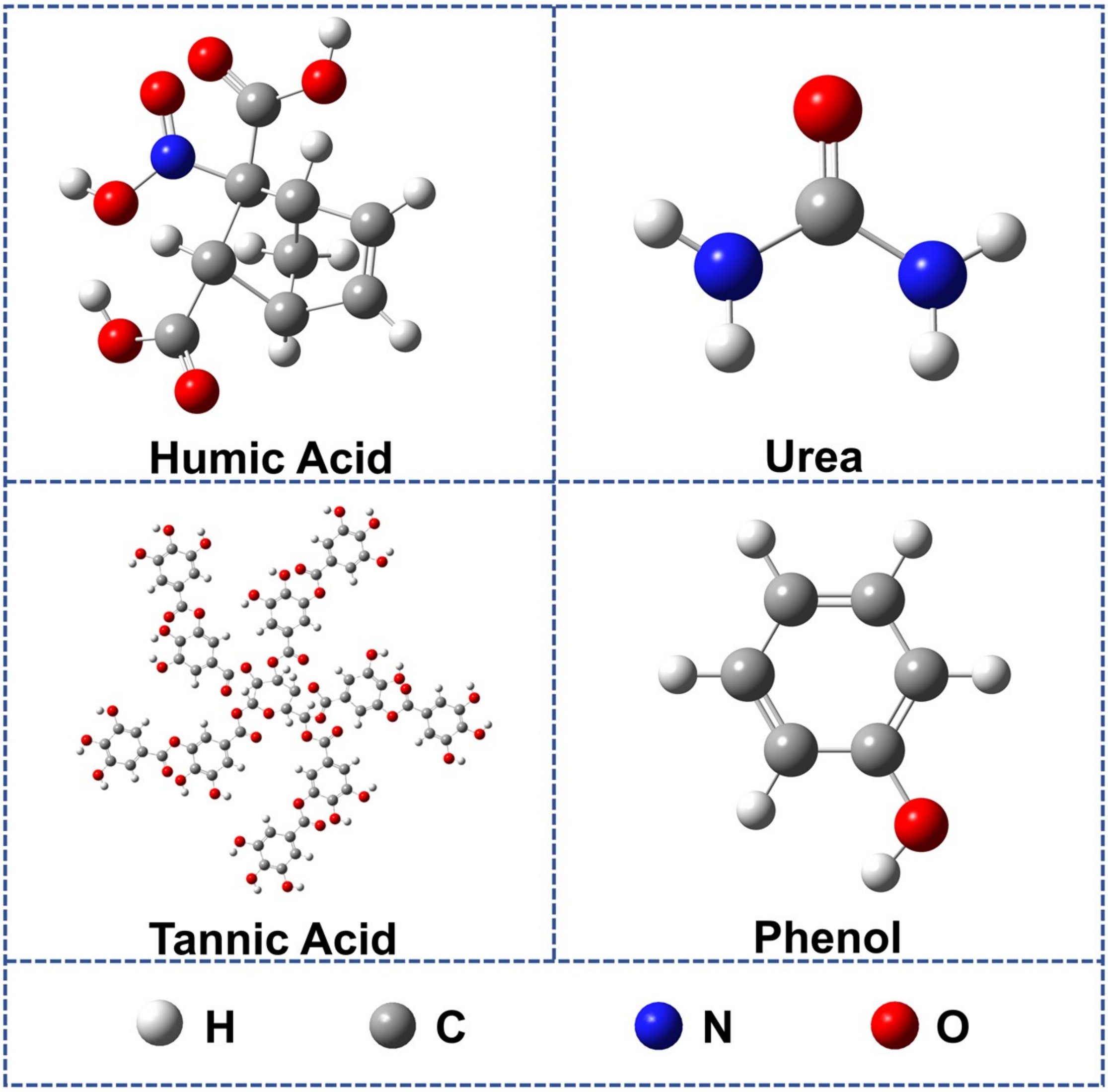

Fig. S5 Molecular structure diagram of organic interfering substances.

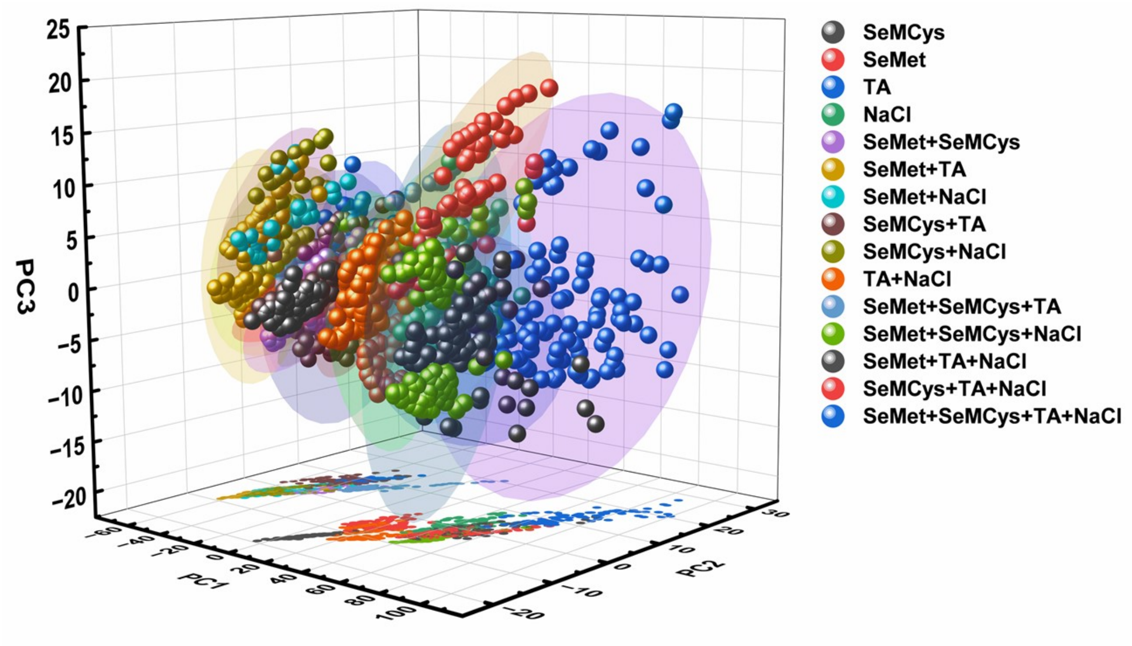

Fig. S6 The 3D-PCA clustering score diagram of mixed organic selenium and interfering substances in well water.

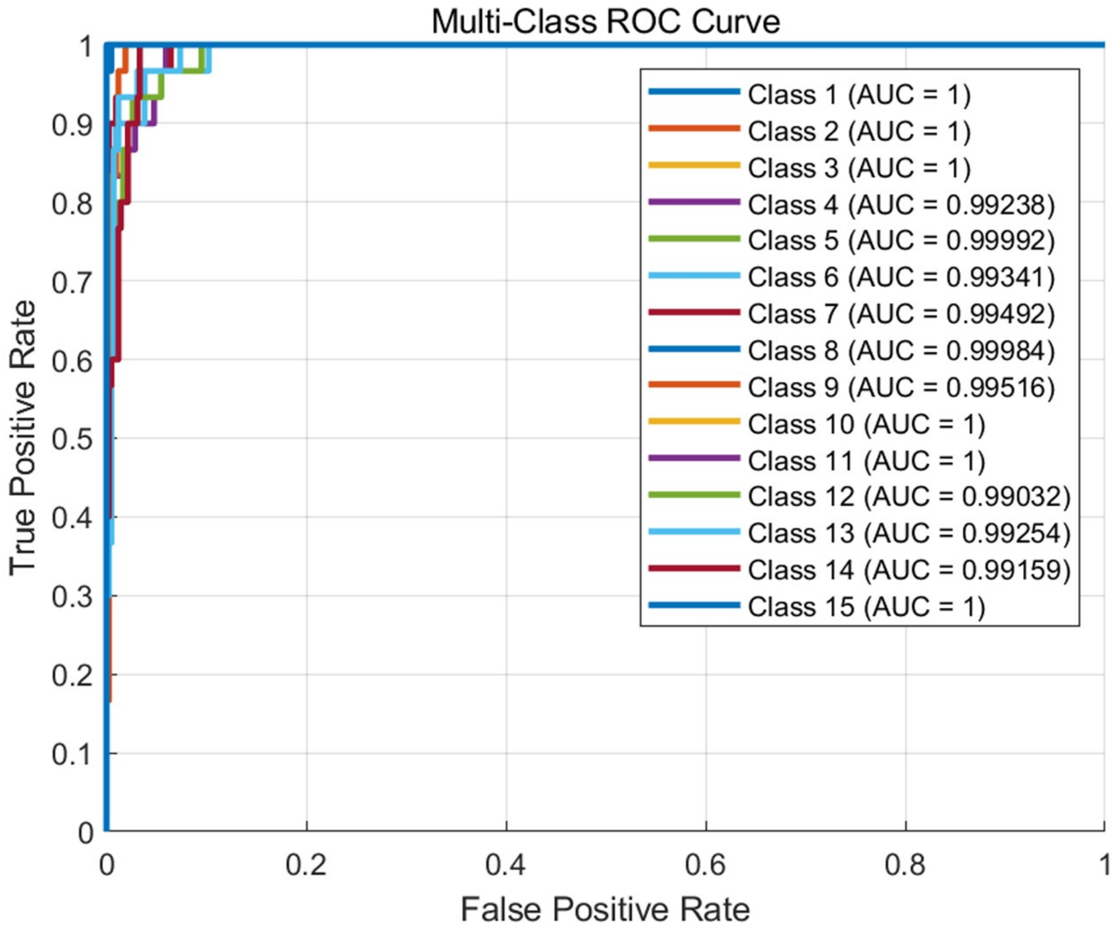

Fig. S7 The ROC curve of the results of the trained SVM model validation set in the well water system.

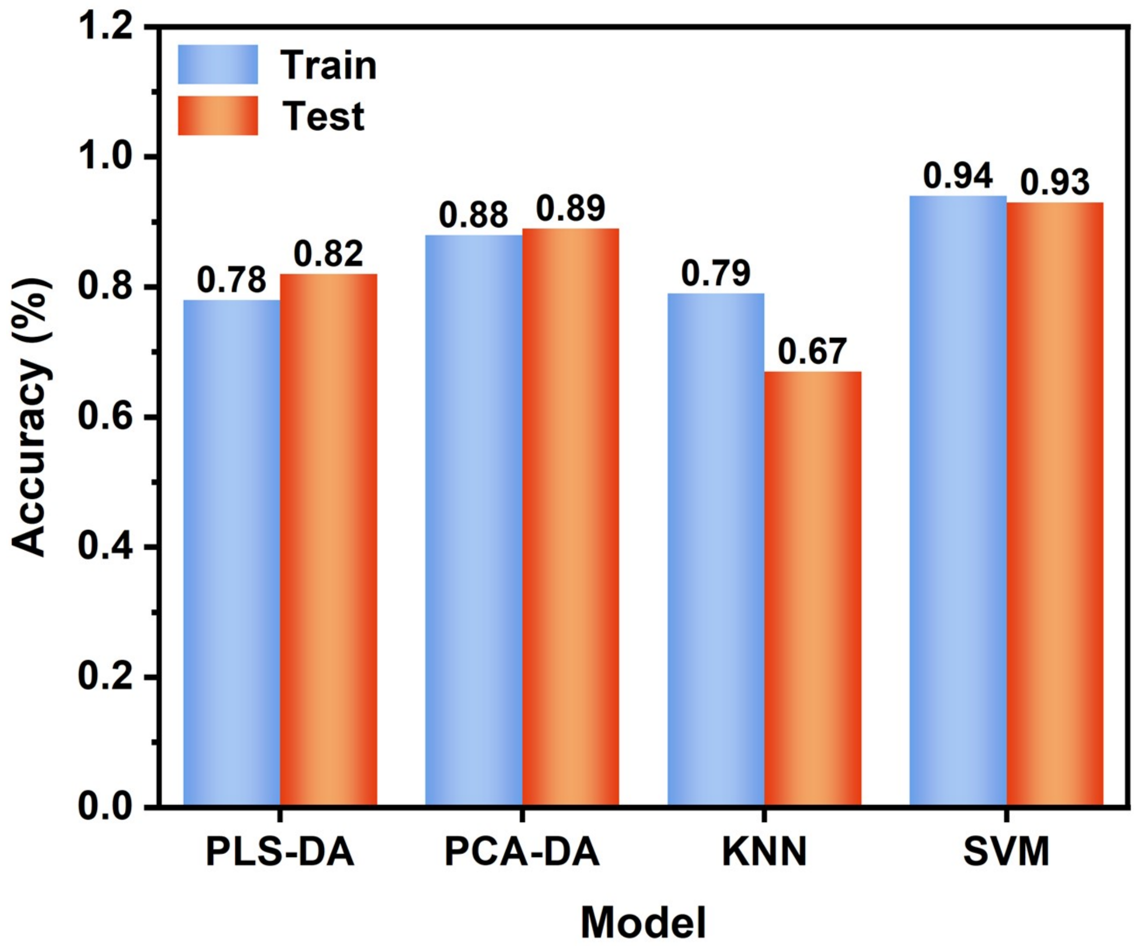

Fig. S8 Classification accuracy of four machine learning models in well water system.

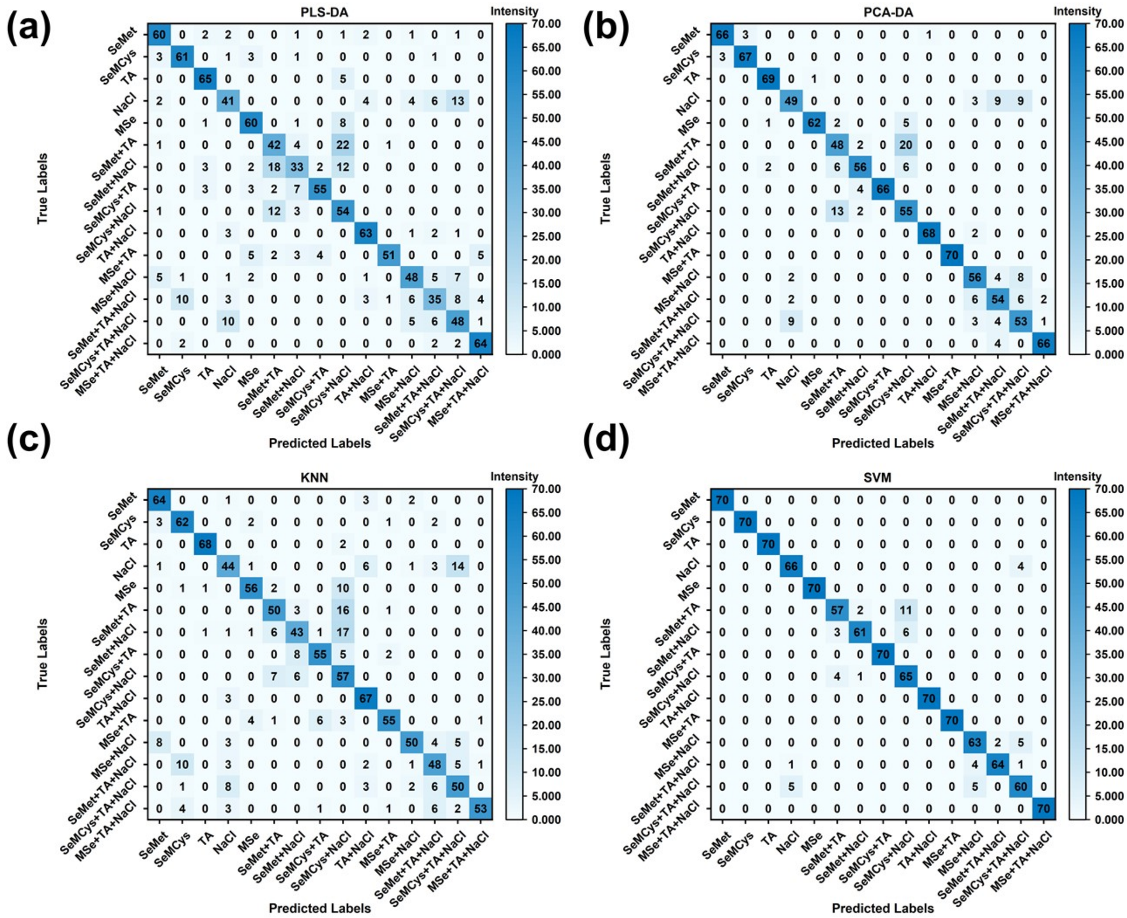

Fig. S9 The training set based on (a) PLS-DA, (b) PCA-DA, (c) KNN and (d) SVM models in well water system.

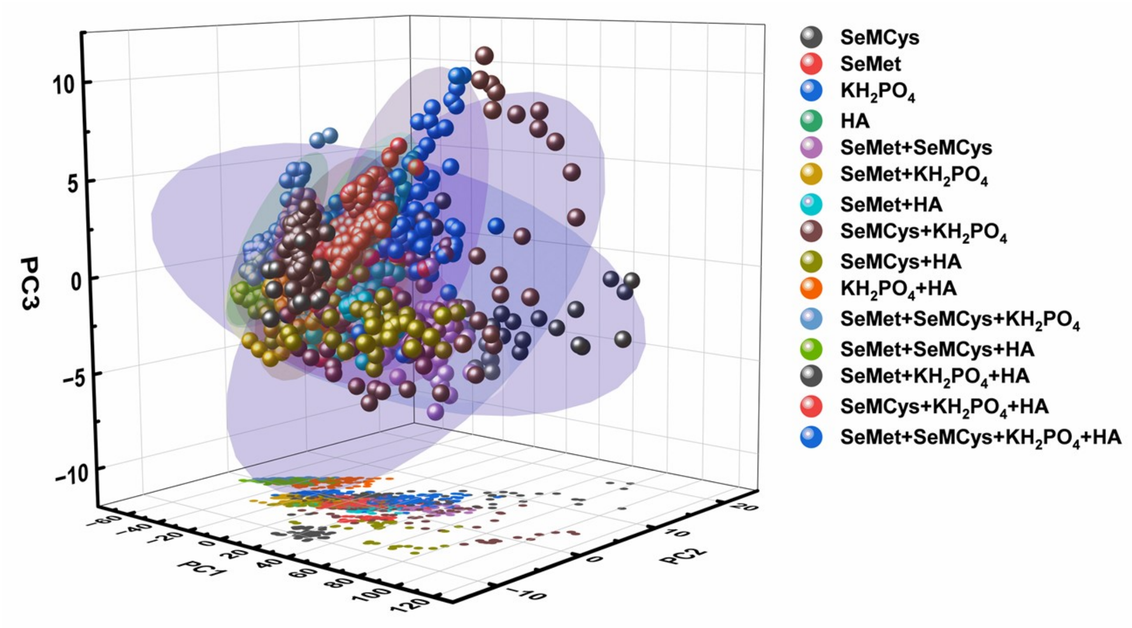

Fig. S10 The 3D-PCA clustering score diagram of mixed organic selenium and interfering substances in soil.

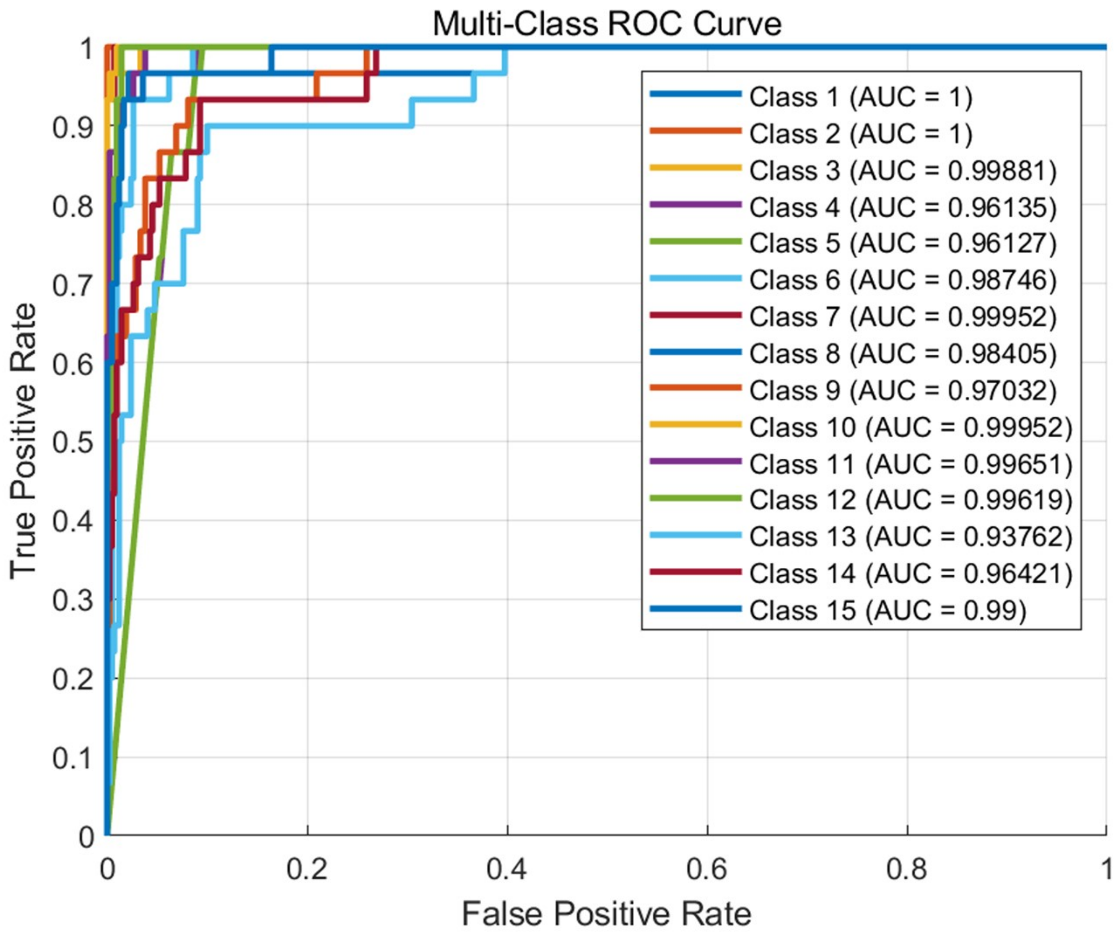

Fig. S11 The ROC curve of the results of the trained SVM model validation set in the soil system.

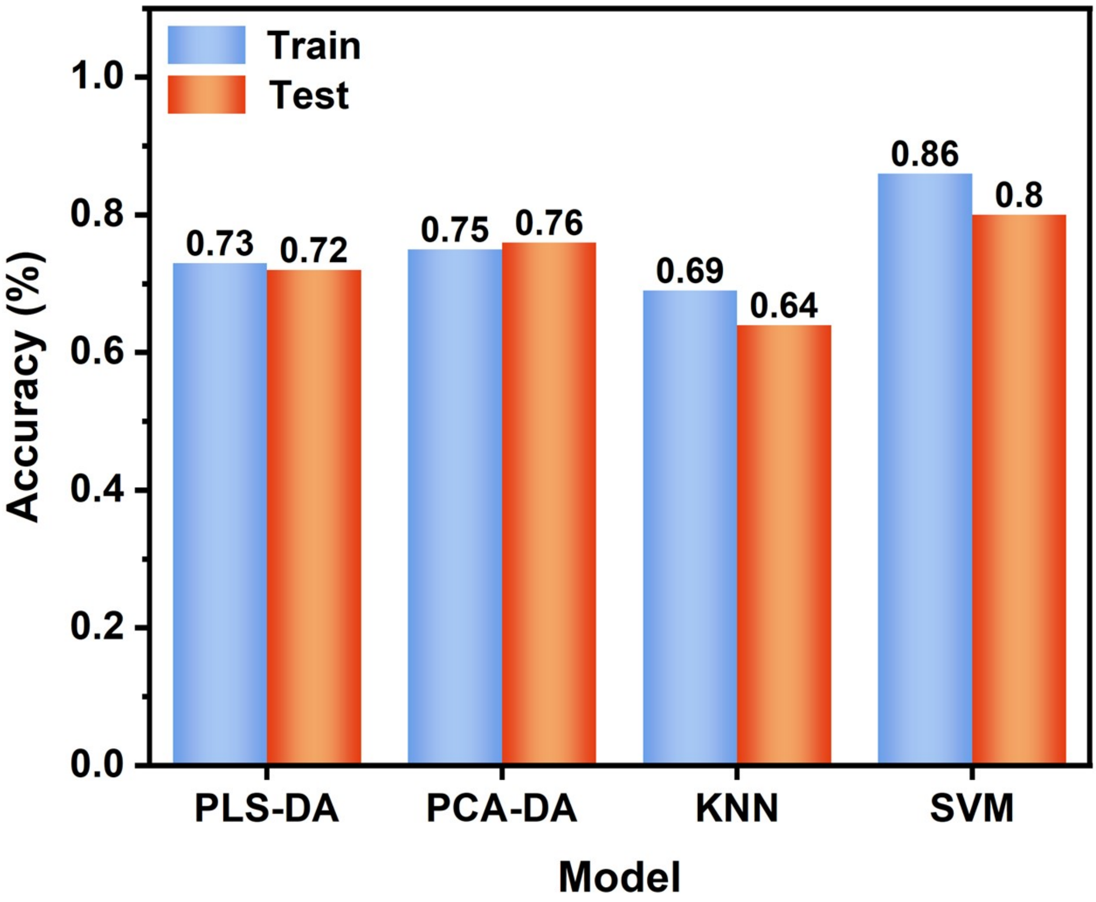

Fig. S12 Classification accuracy of four machine learning models in soil system.

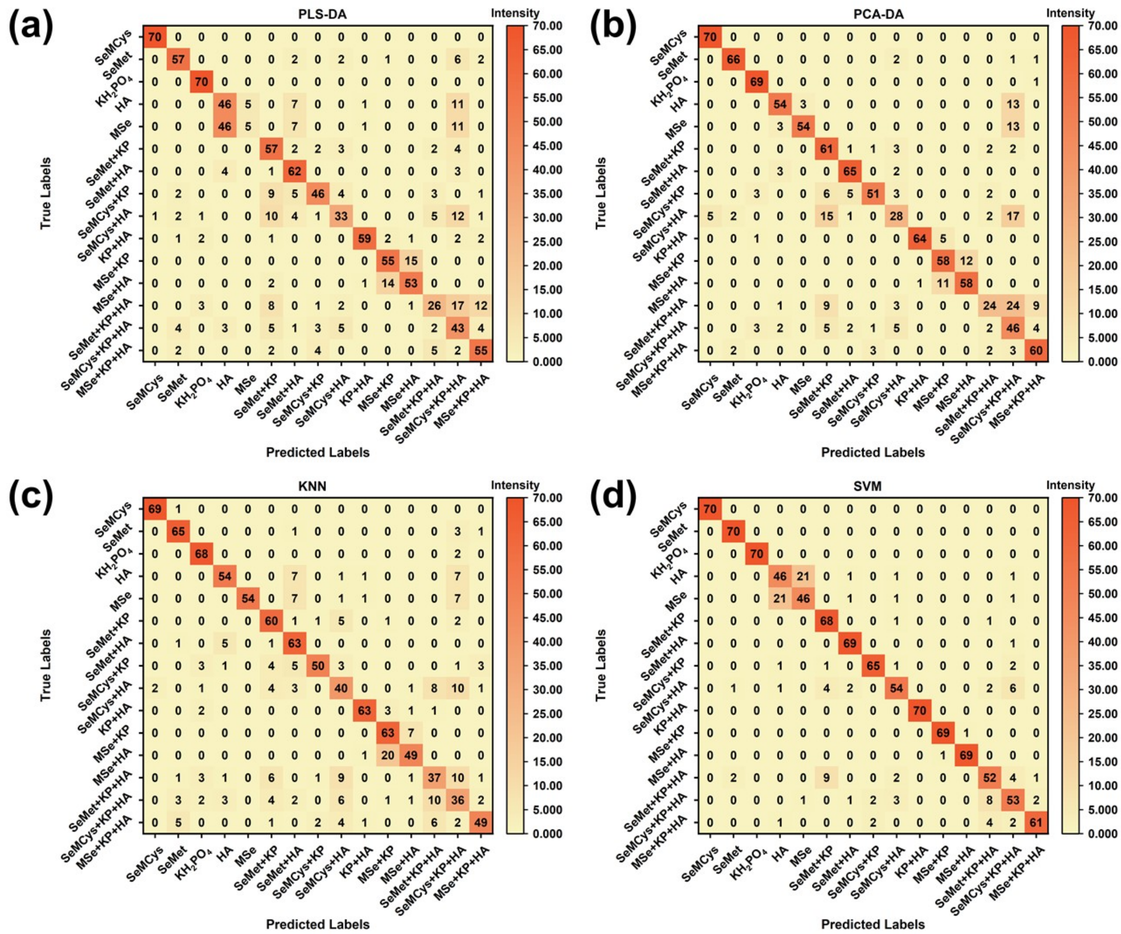

Fig. S13 The training set based on (a) PLS-DA, (b) PCA-DA, (c) KNN and (d) SVM models in soil system.

Table S1 The characteristic peaks and attribution of organic selenium and interfering substances.

Substance	SERS Peak (cm^{-1})	Assignment	Reference
SeMet	640	υ_{as} (Se—CH_2)	1
	827	υ (C—C)	
SeMCys	588	υ (Se—C)	2
	654		
K_2SO_4	988	δ (S=O)	
KH_2PO_4	870	υ (H—O)	3
	1077	υ (P—O)	
$(NH_4)_2HPO_4$	947	υ_s (PO_4^{3-})	
HA	1252	υ (C—O)	4
Urea	1006	υ (C—N)	2
TA	1613	υ (ring, 8a)	5
	1700	υ (C=O)	
Phenol	1002	υ (ring, 1)	6

v-stretching vibration, v_s-symmetric vibration, v_{as}-antisymmetric vibration, δ-bending vibration, ring-aromatic ring.

Table S2 Composition of well water samples.

Composition	ρ (mg/L)	Composition	ρ (mg/L)
K^+	2.918	Cl^-	12.309
Na^+	46.014	SO_4^{2-}	211.320
Ca^+	87.831	HCO_3^-	192.314
Mg^+	27.566	NO_3^-	2.210
SeMet	Not detected	SeMCys	Not detected

Table S3 Composition of soil samples.

Test Items	Unit	Value
pH		8.12
Available phosphorus	mg/kg	14.752
Nitrate nitrogen	mg/kg	135.094
Available potassium	mg/kg	225.426
Ammonium nitrogen	mg/kg	3.956
Organic matter	g/kg	25.139
SeMet	mg/kg	Not detected
SeMCys	mg/kg	Not detected

Table S4 Optimal Parameters for Four Classification Models in Well Water and Soil Samples.

Model	Matrix	Optimal parameters
PLS-DA	Well water	LVs=9.00
	Soil	LVs=12.00
PCA-DA	Well water	PCs=10.00
	Soil	PCs=15.00
KNN	Well water	k=5.00
	Soil	k=7.00
SVM	Well water	C=32.00, γ=0.125
	Soil	C=128.00, γ=0078125

Table S5: Optimal parameters for PLSR and SVR models under different matrices and analytes.

Matrix	Analyte	Model	Optimal parameters
Well water	SeMet	PLSR	LVs=7.00
		SVR	C=8.00, γ=0.03
	SeMCys	PLSR	LVs=6.00
		SVR	C=4.00, γ=0.06
Soil	SeMet	PLSR	LVs=10.00
		SVR	C=64.00, γ=0.02
	SeMCys	PLSR	LVs=9.00
		SVR	C=32.00, γ=0.03

Table S6 Performance comparison of four machine learning models in well water for predicting SERS spectra of single and mixed organic selenium.

		Train sets			Tset sets		
Models	Analytes	sensitivity	specificity	precision	sensitivity	specificity	precision
PLS-DA	SeMet	0.86	0.99	0.83	0.90	0.99	0.87
	SeMCys	0.87	0.99	0.82	0.83	0.99	0.83
	TA	0.93	0.99	0.88	0.97	1.00	0.97
	NaCl	0.59	0.98	0.67	0.70	0.98	0.75
	SeMet+SeMCys (1:1)	0.86	0.98	0.80	0.83	0.99	0.86
	SeMet+TA (1:1)	0.60	0.97	0.55	0.50	0.95	0.41
	SeMet+NaCl (1:1)	0.47	0.98	0.62	0.50	0.98	0.60
	SeMCys+TA (1:1)	0.79	0.99	0.90	0.80	0.99	0.83
	SeMCys+NaCl (1:1)	0.77	0.95	0.53	0.60	0.96	0.53
	TA+NaCl (1:1)	0.90	0.99	0.86	0.97	0.99	0.85
	SeMet+SeMCys+TA (1:1:1)	0.73	1.00	0.96	0.67	0.99	0.83
	SeMet+SeMCys+NaCl (1:1:1)	0.69	0.98	0.74	0.60	0.98	0.64
	SeMet+TA+NaCl (1:1:1)	0.50	0.98	0.61	0.43	0.97	0.54
	SeMCys+TA+NaCl (1:1:1)	0.69	0.97	0.60	0.80	0.97	0.69
	SeMet+SeMCys+TA+NaCl (1:1:1:1)	0.91	0.99	0.86	0.93	0.99	0.88
PCA-DA	SeMet	1.00	0.96	1.00	0.97	1.00	1.00
	SeMCys	1.00	0.96	1.00	0.97	1.00	0.97
	TA	1.00	0.96	1.00	1.00	1.00	0.94
	NaCl	0.99	0.79	0.99	0.80	0.99	0.89
	SeMet+SeMCys (1:1)	1.00	0.98	1.00	0.87	1.00	0.96
	SeMet+TA (1:1)	0.98	0.70	0.98	0.63	0.97	0.61
	SeMet+NaCl (1:1)	0.99	0.88	0.99	0.67	0.99	0.77
	SeMCys+TA (1:1)	1.00	1.00	1.00	0.97	1.00	1.00
	SeMCys+NaCl (1:1)	0.97	0.64	0.97	0.67	0.96	0.57
	TA+NaCl (1:1)	1.00	0.99	1.00	0.97	1.00	0.97
	SeMet+SeMCys+TA (1:1:1)	1.00	1.00	1.00	1.00	1.00	1.00
	SeMet+SeMCys+NaCl (1:1:1)	0.99	0.80	0.99	0.73	0.98	0.76
	SeMet+TA+NaCl (1:1:1)	0.98	0.72	0.98	0.70	0.98	0.75
	SeMCys+TA+NaCl (1:1:1)	0.98	0.70	0.98	0.80	0.97	0.67
	SeMet+SeMCys+TA+NaCl (1:1:1:1)	1.00	0.96	1.00	1.00	1.00	0.97

Continuation Table S6 Performance comparison of four machine learning models in well water for predicting SERS spectra of single and mixed organic selenium.

		Train sets			Tset sets		
Models	Analytes	sensitivity	specificity	precision	sensitivity	specificity	precision
KNN	SeMet	0.91	0.99	0.84	0.93	0.98	0.78
	SeMCys	0.89	0.98	0.79	0.80	0.99	0.86
	TA	0.97	1.00	0.97	0.80	1.00	1.00
	NaCl	0.63	0.98	0.67	0.67	0.98	0.69
	SeMet+SeMCys (1:1)	0.80	0.99	0.88	0.83	0.99	0.89
	SeMet+TA (1:1)	0.71	0.98	0.76	0.53	0.98	0.64
	SeMet+NaCl (1:1)	0.61	0.98	0.72	0.63	0.94	0.43
	SeMCys+TA (1:1)	0.79	0.99	0.87	0.40	0.99	0.71
	SeMCys+NaCl (1:1)	0.81	0.95	0.52	0.80	0.93	0.46
	TA+NaCl (1:1)	0.96	0.99	0.83	0.87	0.98	0.76
	SeMet+SeMCys+TA (1:1:1)	0.79	0.99	0.92	0.67	0.99	0.77
	SeMet+SeMCys+NaCl (1:1:1)	0.71	0.99	0.89	0.53	0.98	0.62
	SeMet+TA+NaCl (1:1:1)	0.69	0.98	0.70	0.47	0.98	0.61
	SeMCys+TA+NaCl (1:1:1)	0.71	0.97	0.66	0.80	0.97	0.63
	SeMet+SeMCys+TA+NaCl (1:1:1:1)	0.76	1.00	0.96	0.63	1.00	0.95
SVM	SeMet	1.00	1.00	1.00	1.00	1.00	1.00
	SeMCys	1.00	1.00	1.00	1.00	1.00	1.00
	TA	1.00	1.00	1.00	1.00	1.00	1.00
	NaCl	0.92	0.94	0.99	0.84	0.90	0.98
	SeMet+SeMCys (1:1)	1.00	1.00	1.00	0.97	1.00	0.99
	SeMet+TA (1:1)	0.89	0.81	0.99	0.93	0.87	0.99
	SeMet+NaCl (1:1)	0.95	0.87	0.99	0.93	0.90	0.99
	SeMCys+TA (1:1)	1.00	1.00	1.00	1.00	0.93	1.00
	SeMCys+NaCl (1:1)	0.79	0.93	0.98	0.85	0.97	0.98
	TA+NaCl (1:1)	1.00	1.00	1.00	1.00	1.00	1.00
	SeMet+SeMCys+TA (1:1:1)	1.00	1.00	1.00	1.00	1.00	1.00
	SeMet+SeMCys+NaCl (1:1:1)	0.88	0.90	0.99	0.83	0.83	0.98
	SeMet+TA+NaCl (1:1:1)	0.97	0.91	0.99	0.85	0.77	0.99
	SeMCys+TA+NaCl (1:1:1)	0.86	0.86	0.98	0.80	0.80	0.98
	SeMet+SeMCys+TA+NaCl (1:1:1:1)	1.00	1.00	1.00	0.97	1.00	0.99

Table S7 Performance comparison of four machine learning models in soil for predicting SERS spectra of single and mixed organic selenium.

		Train sets			Tset sets		
Models	Analytes	sensitivity	specificity	precision	sensitivity	specificity	precision
PLS-DA	SeMCys	1.00	1.00	0.99	1.00	1.00	1.00
	SeMet	0.81	0.99	0.84	0.80	0.99	0.83
	KH_2PO_4	1.00	0.99	0.92	0.97	0.98	0.81
	HA	0.66	0.95	0.46	0.80	0.94	0.47
	SeMet+SeMCys (1:1)	0.07	0.99	0.50	0.03	1.00	0.33
	SeMet+KH_2PO_4 (1:1)	0.81	0.96	0.60	0.83	0.97	0.64
	SeMet+HA (1:1)	0.89	0.97	0.69	0.83	0.97	0.64
	SeMCys+KH_2PO_4 (1:1)	0.66	0.99	0.81	0.33	1.00	0.91
	SeMCys+HA (1:1)	0.47	0.98	0.67	0.43	0.97	0.54
	KH_2PO_4+HA (1:1)	0.84	1.00	0.95	0.70	1.00	0.95
	SeMet+SeMCys+KH_2PO_4 (1:1:1)	0.79	0.98	0.76	0.63	0.97	0.63
	SeMet+SeMCys+HA (1:1:1)	0.76	0.98	0.76	0.67	0.97	0.59
	SeMet+KH_2PO_4+HA (1:1:1)	0.37	0.98	0.6	0.50	0.98	0.62
	SeMCys+KH_2PO_4+HA (1:1:1)	0.61	0.93	0.39	0.50	0.92	0.31
	SeMet+SeMCys+KH_2PO_4+HA (1:1:1:1)	0.79	0.98	0.71	0.73	0.98	0.76
PCA-DA	SeMCys	1.00	0.99	0.93	1.00	1.00	1.00
	SeMet	0.94	1.00	0.94	1.00	1.00	0.97
	KH_2PO_4	0.99	0.99	0.91	0.93	1.00	0.97
	HA	0.77	0.94	0.47	0.77	0.94	0.47
	SeMet+SeMCys (1:1)	0.74	0.94	0.5	0.7	0.99	0.5
	SeMet+KH_2PO_4 (1:1)	0.87	0.96	0.64	0.93	0.97	0.68
	SeMet+HA (1:1)	0.93	0.99	0.88	0.93	0.98	0.8
	SeMCys+KH_2PO_4 (1:1)	0.73	0.99	0.91	0.43	1.00	0.87
	SeMCys+HA (1:1)	0.4	0.98	0.61	0.43	0.97	0.54
	KH_2PO_4+HA (1:1)	0.91	1.00	0.98	0.87	1.00	0.93
	SeMet+SeMCys+KH_2PO_4 (1:1:1)	0.83	0.98	0.78	0.8	0.98	0.77
	SeMet+SeMCys+HA (1:1:1)	0.83	0.99	0.83	0.87	0.98	0.79
	SeMet+KH_2PO_4+HA (1:1:1)	0.34	0.99	0.71	0.47	0.99	0.82
	SeMCys+KH_2PO_4+HA (1:1:1)	0.66	0.93	0.39	0.67	0.93	0.41
	SeMet+SeMCys+KH_2PO_4+HA (1:1:1:1)	0.86	0.98	0.8	0.8	0.98	0.75

Continuation Table S7 Performance comparison of four ML models soil water for predicting SERS spectra of single and mixed organic selenium.

		Train sets			Tset sets		
Models	Analytes	sensitivity	specificity	precision	sensitive	specificity	precision
KNN	SeMCys	0.99	1.00	0.97	0.97	1.00	1.00
	SeMet	0.93	0.99	0.86	0.9	0.99	0.84
	KH_2PO_4	0.97	0.99	0.86	0.93	0.99	0.85
	HA	0.77	0.93	0.46	0.73	0.94	0.48
	SeMet+SeMCys (1:1)	0.77	1.00	0.46	0.73	1.00	0.48
	SeMet+KH_2PO_4 (1:1)	0.86	0.98	0.75	0.87	0.96	0.62
	SeMet+HA (1:1)	0.9	0.97	0.71	0.97	0.95	0.56
	SeMCys+KH_2PO_4 (1:1)	0.71	1.00	0.93	0.33	1.00	0.91
	SeMCys+HA (1:1)	0.57	0.97	0.58	0.37	0.98	0.55
	KH_2PO_4+HA (1:1)	0.9	1.00	0.94	0.9	1.00	0.93
	SeMet+SeMCys+KH_2PO_4 (1:1:1)	0.9	0.97	0.72	0.53	0.98	0.7
	SeMet+SeMCys+HA (1:1:1)	0.7	0.99	0.82	0.77	0.95	0.55
	SeMet+KH_2PO_4+HA (1:1:1)	0.53	0.97	0.6	0.4	1.00	0.92
	SeMCys+KH_2PO_4+HA (1:1:1)	0.51	0.96	0.45	0.63	0.94	0.44
	SeMet+SeMCys+KH_2PO_4+HA (1:1:1:1)	0.70	0.99	0.86	0.8	0.97	0.69
SVM	SeMCys	1.00	1.00	1.00	0.93	1.00	1.00
	SeMet	1.00	0.99	0.96	0.97	1.00	0.97
	KH_2PO_4	1.00	1.00	1.00	0.607	0.997	0.47
	HA	0.63	0.98	0.47	0.63	0.98	0.50
	SeMet+SeMCys (1:1)	0.66	0.95	0.49	0.90	0.95	0.69
	SeMet+KH_2PO_4 (1:1)	0.97	0.99	0.83	0.97	0.97	0.88
	SeMet+HA (1:1)	0.99	0.99	0.93	0.87	0.99	0.93
	SeMCys+KH_2PO_4 (1:1)	0.93	0.99	0.94	0.67	0.99	0.74
	SeMCys+HA (1:1)	0.77	0.99	0.86	0.93	0.98	0.93
	KH_2PO_4+HA (1:1)	1.00	1.00	1.00	0.93	0.99	0.93
	SeMet+SeMCys+KH_2PO_4 (1:1:1)	0.99	0.99	0.99	0.88	0.99	0.87
	SeMet+SeMCys+HA (1:1:1)	0.985	0.998	0.985	0.67	0.99	0.57
	SeMet+KH_2PO_4+HA (1:1:1)	0.74	0.98	0.78	0.67	0.96	0.65
	SeMCys+KH_2PO_4+HA (1:1:1)	0.76	0.98	0.76	0.80	0.97	0.86
	SeMet+SeMCys+KH_2PO_4+HA (1:1:1:1)	0.87	0.99	0.95	0.93	1.00	1.00

References

1 E.J. Baran, Zeitschrift Für Naturforschung B., 2005 60. https://doi.org/10.1515/znb-2005-0609

2 J. Lopez, T.C. Jao and W.E. Rudzinski, J. Inorg. Biochem., 1981, 14, 177-188. https://doi.org/10.1016/s0162-0134(00)80038-0

3 J. Li, Y. Ma, J. Zhang and D. Kong, Spectrochimica Acta Part a: Molecular and Biomolecular Spectroscopy, 2025, 324, 124985. https://doi.org/10.1016/j.saa.2024.124985

4 M.L. Roldán, G. Corrado, O. Francioso and S. Sánchez-Cortés, Anal. Chim. Acta., 2011, 699, 87-95, https://doi.org/10.1016/j.aca.2011.05.001

5 A. Espina, M.V. Cañamares, Z. Jurasekova and S. Sanchez-Cortes, Acs Omega., 2022, 7, 27937-27949. https://doi.org/10.1021/acsomega.2c01679

6 M. Garncarzová, L. Veselý, B. Kim, K. Kim and D. Heger, Spectrochimica Acta Part a: Molecular and Biomolecular Spectroscopy, 2025, 335, 125948. https://doi.org/10.1016/j.saa.2025.125948